PHYSICAL REVIEW A VOLUME 8, NUMBER 4 OCTOBER 1973

Yield Ratios, $K\alpha/K\beta$, $L\alpha/L\beta$, $L\alpha/L\gamma$, and $L\alpha/Ll$, for X Rays Produced by Protons of 1.0 to 3.7 MeV†

D. A. Close, R. C. Bearse,* J. J. Malanify, and C. J. Umbarger
Nuclear Analysis Research Group, University of California, Los Alamos Scientific Laboratory, Los Alamos, New Mexico 87544
(Received 30 May 1973)

$K\alpha/K\beta$ x-ray yield ratios have been determined for eleven elements, Ti, V, Fe, Ni, Cu, Ge, Rb, Zr, Ag, Sn, and Sb, when bombarded with protons of 1.00, 2.25, and 3.00 MeV. Excitation functions of $K\alpha/K\beta$ ratios for Ni, Ge, and Ag were also measured from 1.00 to 3.70 MeV in 100-keV steps, and these ratios were found to be constant with proton energy. For the ten elements Ce, Sm, Dy, Tm, W, Au, Pb, Bi, Th, and U, the yield ratios $L\alpha/L\beta$, $L\alpha/L\gamma$, and $L\alpha/Ll$ were determined for proton bombarding energies of 1.00, 2.25, and 3.00 MeV. Excitation functions for these same ratios were measured for Sm, W, and Th for proton energies between 1.00 and 3.70 MeV in 100-keV steps. While the $L\alpha/L\beta$ and $L\alpha/L\gamma$ ratios varied significantly with proton energy, the $L\alpha/Ll$ ratio was found to be constant as a function of proton energy. Additionally, the energy of the centroid of the peak corresponding to the $L\alpha$, $L\beta$, and $L\gamma$ x-ray transitions was measured as a function of proton energy for Sm, W, and Th. The $L\beta$ and $L\gamma$ centroid energies changed appreciably with proton energy, while the $L\alpha$ centroid energy remained constant. The experimental yield ratios and centroid energies are compared to plane-wave-Born- and binary-encounter-approximation predictions.

I. INTRODUCTION

To complement our earlier paper[1] concerning $K\alpha$ or $L\alpha$ x-ray production cross sections measured for proton energies between 1.00 and 3.70 MeV for 21 elements, and to provide more detailed data to better check existing theories pertaining to proton-induced x-ray fluorescence, we now report on $K\alpha/K\beta$, $L\alpha/L\beta$, $L\alpha/L\gamma$, and $L\alpha/Ll$ yield ratios determined for those same elements. The ratios are compared to the theoretical predictions of the binary-encounter approximation (BEA) of Garcia[2,3] and the plane-wave Born approximation (PWBA) of Merzbacher and collaborators.[4] We also report determinations of $L\alpha$, $L\beta$, and $L\gamma$ x-ray centroid energies as a function of proton energy.

II. EXPERIMENTAL TECHNIQUE

As described in Ref. 1, 21 targets were obtained[5] either as self-supporting foils or as films evaporated onto 40 $\mu g/cm^2$ carbon backings. The targets were mounted in a chamber[6] designed for elemental analysis and bombarded by protons from the Los Alamos Scientific Laboratory 3.75-MV Van de Graaff. The detector was a Si(Li) detector having a 0.025-mm thick Be window and a resolution of 175 eV at 5.9 keV, which viewed the target at 90° from the beam direction. In reaching the detector, the x-rays traversed a 0.013-mm Mylar window and a 4.1-cm air path. Absorbers were inserted into this path to reduce x-ray counting rates so that dead-time corrections were less than 1%. The effect of each attenuator was determined to an accuracy better than 2% for each radiation measured. The x-ray detection efficiency was measured using the method described by Bissinger[7] and in Ref. 1. The relative efficiency as a function of x-ray energy was measured using ^{241}Am, ^{109}Cd, and ^{57}Co sources.[8,9] The over-all efficiency was determined by correcting for the effects of the Mylar window, the air path, x-ray absorbers, and the attenuation in the target itself. The energy calibration was also based on these sources.[10]

Figure 1 shows x-ray spectra produced by Sm and Th when fluoresced by 2.25-MeV protons. The principal subgroups in each spectrum are labeled. In general, the subgroups were very well resolved and easily integrated; background subtraction was performed in each case by straight-line interpolation. For the lightest elements, however, a two-Gaussian fitting routine was used for subgroup intensity determination.

III. RESULTS

The $K\alpha/K\beta$ yield ratios measured for the eleven elements are plotted in Fig. 2 and are listed in Table I for comparison with the data of Slivinsky *et al.*,[11] Hansen *et al.*,[12] and Rao *et al.*[13] The data of Rao are a best fit to available experimental data. The agreement of the present data with the other reported works in Table I is, in general, within the stated error of each measurement. The major exceptions are the $K\alpha/K\beta$ ratios for Ti and V from Hansen *et al.*, where the two sets of results fall considerably outside stated error bars. Our results for Ti and V are, however, in good

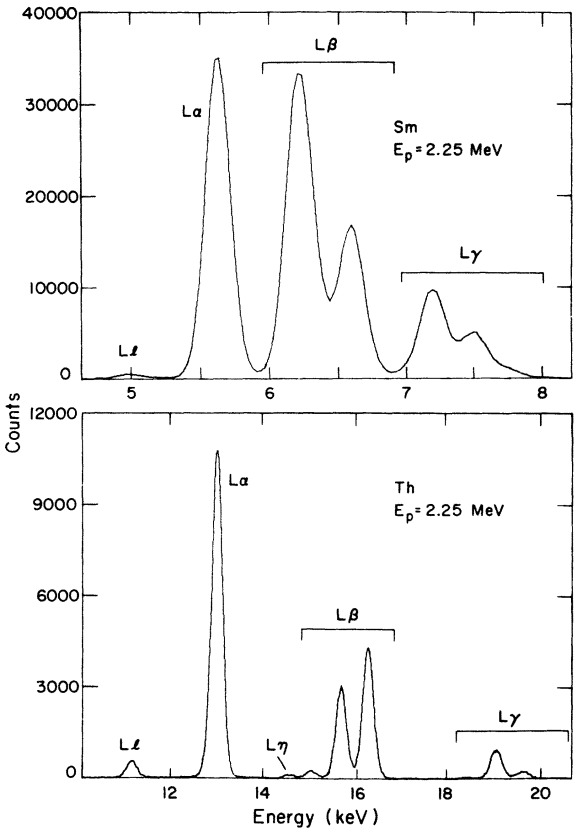

FIG 1. Typical x-ray spectra for Sm and Th fluoresced by 2.25 MeV protons. The major L subgroups are labeled.

TABLE I. $K\alpha/K\beta$ yield ratios vs atomic number.

Z	Element	$K\alpha/K\beta$ [a]	$K\alpha/K\beta$ [b]	$K\alpha/K\beta$ [c]	$K\alpha/K\beta$ [d]	$K\alpha/K\beta$ [e]
22	Ti	7.57	7.58	10.58	7.52	
23	V	7.40	7.47	9.50	7.52	
26	Fe	7.36	7.32	7.79	7.46	
28	Ni	6.97	7.22	7.53	7.41	
29	Cu	7.43	7.21	7.47	7.41	
32	Ge	6.77	6.70	7.17	6.76	
37	Rb	5.62		5.95	5.80	
40	Zn	5.22		5.44	5.41	
47	Ag	4.61		4.74	4.74	4.68 ± 0.33
50	Sn	4.46		4.49	4.55	
51	Sb	4.42		4.44	4.48	

[a] Present work, standard deviation ± 5%.
[b] Slivinsky *et al.*, Ref. 11, standard deviation ± 1%.
[c] Hansen *et al.*, Ref. 12, standard deviation ± 2%.
[d] Rao *et al.*, Ref. 13.
[e] Bissinger *et al.*, Ref. 7

agreement with those of Slivinsky[11] and Rao.[13] The $K\alpha/K\beta$ ratio for Ag from the work of Bissinger *et al.*[7] is also included in Table I and agrees to within 2% of our value. The present measurements and those of Bissinger *et al.*[7] were taken using proton excitation, whereas the other results in Table I were taken using photon and electron excitation. Thus, the $K\alpha/K\beta$ ratios seem independent of the excitation mechanism so long as multiple ionization does not occur. Figure 3 shows the invariance of the $K\alpha/K\beta$ ratios for Ni, Ge, and Ag as a function of proton energy from 1.00 to 3.70 MeV. In order to be more quantitative concerning the independence of the $K\alpha/K\beta$ ratios with energy, a linear least-squares fit to the Ag $K\alpha/K\beta$ ratio measurements between 1.00 and 3.70 MeV was performed. The fit showed that the slope of a straight line through the data points (see Fig. 3) was not significantly different from zero at the 95% confidence level. This constancy is expected,

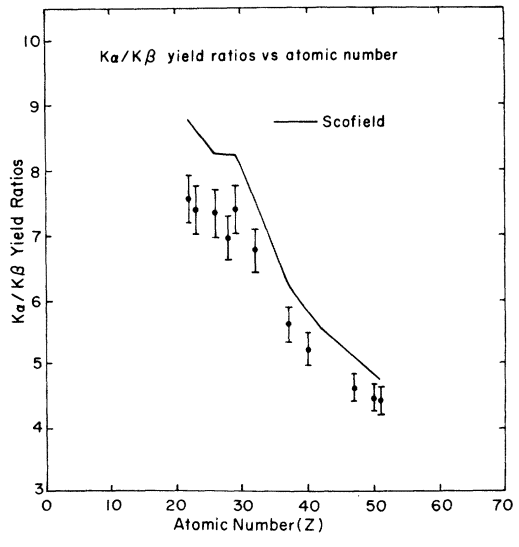

FIG. 2. $K\alpha/K\beta$ yield ratios plotted vs atomic number. The theoretical calculations of Scofield are included for comparison.

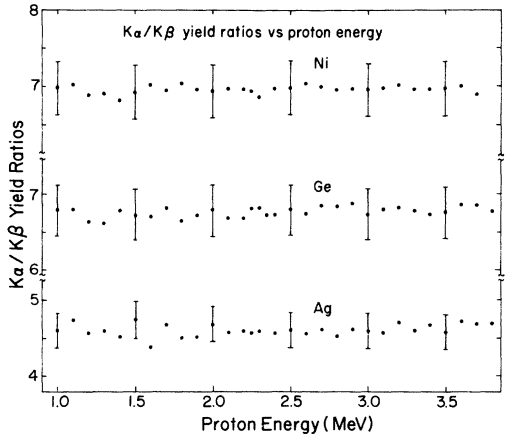

FIG. 3. $K\alpha/K\beta$ yield ratios plotted vs proton energy for Ni, Ge, and Ag

TABLE II. $L\alpha/L\beta$,[a] $L\alpha/L\gamma$,[a] and $L\alpha/Ll$[b] yield ratios vs proton energy and atomic number.

		1.00 MeV		2.25 MeV		3.00 MeV		
Z	Element	$L\alpha/L\beta$	$L\alpha/L\gamma$	$L\alpha/L\beta$	$L\alpha/L\gamma$	$L\alpha/L\beta$	$L\alpha/L\gamma$	$L\alpha/Ll$
58	Ce	1.68	12.4	1.56	10.1	1.49	9.28	23.3
62	Sm	1.83	14.5	1.47	8.96	1.39	7.94	22.5
66	Dy	1.82	14.6	1.50	10.2	1.47	9.18	23.4
69	Tm	1.76	14.2	1.52	10.3	1.42	9.11	25.3
74	W	1.88	13.9	1.62	10.7	1.52	9.44	20.9
79	Au	1.89	14.0	1.72	11.9	1.67	11.5	21.0
82	Pb	2.11	12.7	1.84	10.5	1.75	10.0	18.6
83	Bi	1.93	12.9	1.71	11.2	1.66	10.2	20.1
90	Th	1.92	11.5	1.82	10.7	1.73	9.78	17.2
92	U	2.02	11.3	1.93	10.5	1.79	9.44	17.3

[a] Standard deviation ±5%, except Ce and Sm, which are ±10% and ±7%, respectively.
[b] Standard deviation ±15%, except Ce and Sm, which are ±20%.

assuming nonmultiple ionization, since both the $K\alpha$ and $K\beta$ transitions arise from the filling of a vacancy in the $1s\frac{1}{2}$ shell.

The $L\alpha/L\beta$ and $L\alpha/L\gamma$ ratios for the ten elements bombarded with 1.00, 2.25, and 3.00 MeV protons are shown in Table II. Figures 4 and 5, respectively, show these same ratios plotted versus atomic number. Also shown in Table II are the $L\alpha/Ll$ yield ratios determined from this work. These $L\alpha/Ll$ values are plotted in Fig. 6 versus atomic number. Figures 7 and 8 show the $L\alpha/L\beta$ and $L\alpha/L\gamma$ yield ratios, respectively, plotted versus proton energy for Sm, W, and Th. Figure 9 is a plot of the $L\alpha/Ll$ ratios for W and Th which, within the experimental uncertainty, are constant with proton energy. The average values of these data are reported in Table II. The $L\alpha/Ll$ ratios of the other eight elements also show this energy independence. As with the $K\alpha/K\beta$ ratios, this is expected because both the $L\alpha$ and Ll x-rays result solely from the filling of a vacancy in the same subshell, the $L3$ subshell.

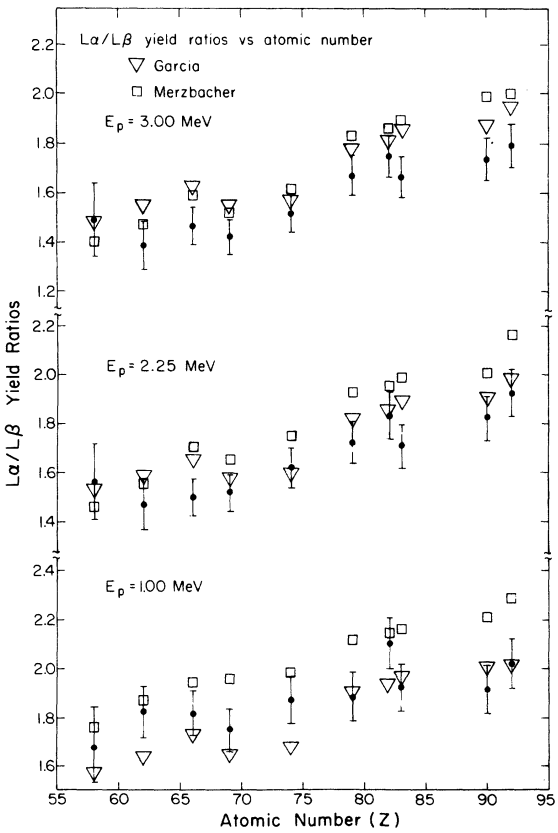

FIG. 4. $L\alpha/L\beta$ yield ratios plotted vs atomic number for 1.00, 2.25, and 3.00 MeV protons. The BEA and PWBA predictions of Garcia and Merzbacher, respectively, are included for comparison.

Results for the $L\alpha/L\beta$ and $L\alpha/L\gamma$ ratios have been reported by Shafroth[14,15] for Au bombarded by protons. Our result for Au $L\alpha/L\beta$ is 6% higher than those results at 1.00 and 3.00 MeV. For $L\alpha/L\gamma$ our results are 10% and 20% higher at 1.00 and 3.00 MeV, respectively.

Results[16] for $L\alpha/L\beta$ from Pb are within 3% of our results at both 1.00 and 3.00 MeV. For the $L\alpha/L\gamma$ ratios, however, our values are 34% and 18% lower at 1.00 and 3.00 MeV, respectively, considerably outside stated errors. For the $L\alpha/Ll$ ratio, our result is within 3% of the average of Ref. 16 values between 1.00 and 3.00 MeV. Busch *et al.*[16] report an increase in the $L\alpha/Ll$ ratio for Pb from 1.00 and 3.00 MeV which we fail to see. Within experimental uncertainty, we also see no change in the $L\alpha/Ll$ ratios for any of the other nine elements investigated here, taking note that our experimental uncertainty lies between 15 and 20% for these measurements.

Figures 10–12 show the $L\alpha$, $L\beta$, and $L\gamma$ centroid energies plotted versus proton energy. The

figures show the change in centroid energy with proton energy for the $L\beta$ and $L\gamma$ subgroups, as reported earlier.[15,16] This arises because the individual subshell cross sections vary differently with proton energy, and each $L\beta$ and $L\gamma$ subgroup is made up of components arising from more than one subshell. This involvement of more than one subshell is also responsible for the variations with energy of the $L\alpha/L\beta$ and $L\alpha/L\gamma$ yield ratios. On the other hand, the $L\alpha$ centroid energy remains constant with proton energy due to the fact that the $L\alpha$ subgroup originates from a vacancy in only one subshell, $L3$.

IV. COMPARISON WITH THEORY

Using the method of Ref. 14, the yield ratios of $L\alpha/L\beta$, $L\alpha/L\gamma$, and $L\alpha/Ll$ can be calculated theoretically using appropriate subshell-ionization cross sections and the following intensity equations:

$$I_{L\alpha} = \{[n_1(f_{13}+f_{12}f_{23})+n_2f_{23}+n_3]\omega_3\}F_{3\alpha}\,, \tag{1}$$

$$I_{L\beta} = n_1\omega_1F_{1\beta}+(n_1f_{12}+n_2)\omega_2F_{2\beta} + [n_1(f_{13}+f_{12}f_{23})+n_2f_{23}+n_3]\omega_3F_{3\beta}\,, \tag{2}$$

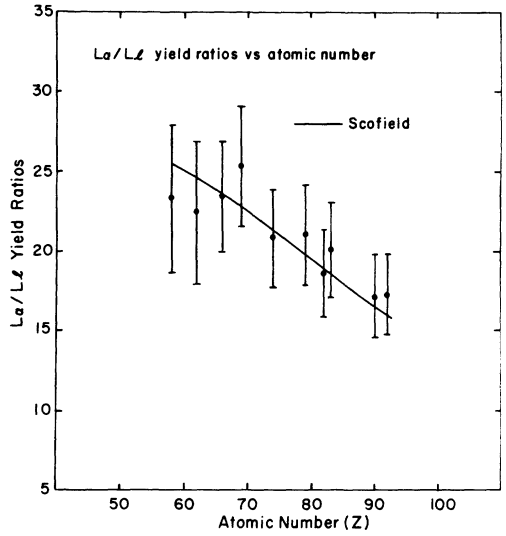

FIG. 6. $L\alpha/Ll$ yield ratios plotted vs atomic number. The theoretical calculations of Scofield are also included.

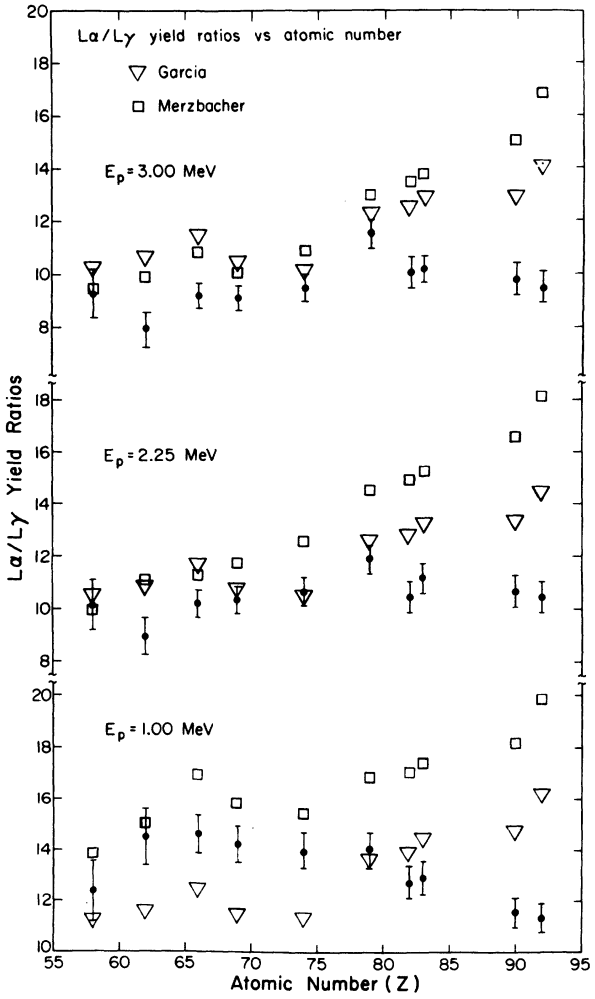

FIG. 5 $L\alpha/L\gamma$ yield ratios plotted vs atomic number for 1.00, 2.25, and 3.00 MeV protons. The BEA and PWBA predictions of Garcia and Merzbacher, respectively, are included for comparison.

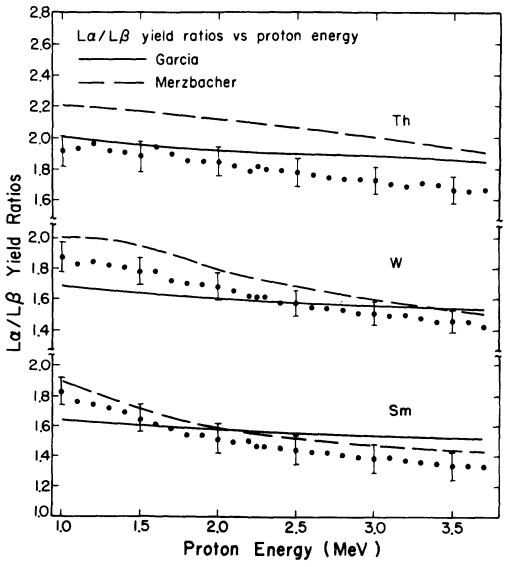

FIG. 7. $L\alpha/L\beta$ yield ratios plotted vs proton energy for Sm, W, and Th. The BEA and PWBA predictions of Garcia and Merzbacher, respectively, are included for comparison.

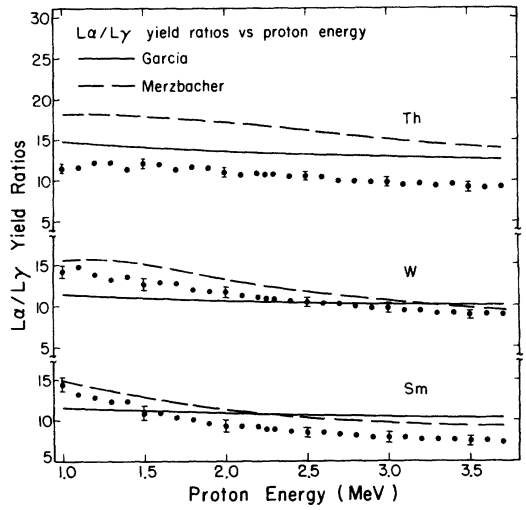

FIG. 8. $L\alpha/L\gamma$ yield ratios plotted vs proton energy for Sm, W, and Th. The BEA and PWBA predictions of Garcia and Merzbacher, respectively, are included for comparison.

and

$$I_{L\gamma} = n_1\omega_1 F_{1\gamma} + (n_1 f_{12} + n_2)\omega_2 F_{2\gamma} \ , \tag{3}$$

$$I_{Ll} = \{[n_1(f_{13} + f_{12}f_{23}) + n_2 f_{23} + n_3]\omega_3\} F_{3l} \ , \tag{4}$$

where

$$n_1 = \sigma_{L1}/\sigma_{L3} \ ,$$

$$n_2 = \sigma_{L2}/\sigma_{L3} \ ,$$

$$n_3 = 1 \ ,$$

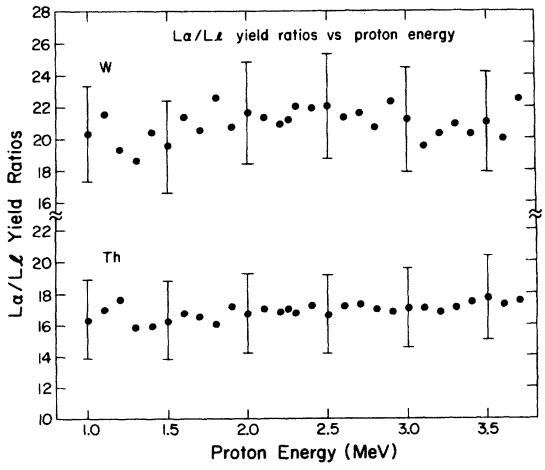

FIG. 9 $L\alpha/Ll$ yield ratios plotted vs proton energy for W and Th.

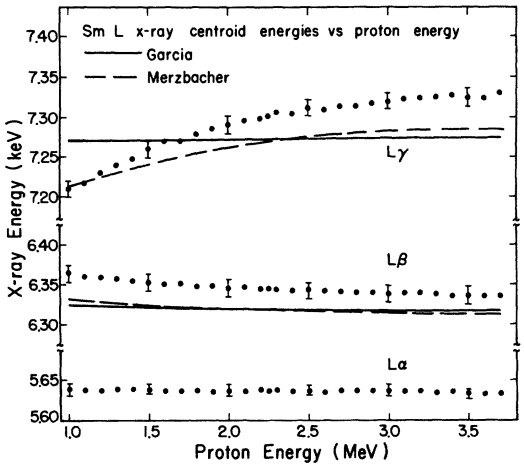

FIG. 10. $L\alpha$, $L\beta$, and $L\gamma$ centroid energies plotted vs proton energy for Sm. The BEA and PWBA predictions of Garcia and Merzbacher, respectively, are included for comparison.

and σ_{Li} is the theoretical ionization cross section for the ith subshell, obtained here from either the PWBA[4] or BEA.[2,3,17] The values of the Koster-Kronig yields (f_{12}, f_{13}, and f_{23}) were obtained from the calculated graphs of Crasemann *et al.*[18] and Chen *et al.*,[19] as were the values of the subshell fluorescence yields (ω_1, ω_2, and ω_3). The F_{ij}'s in Eqs. (1)–(4) were obtained from the work of Schofield[20] and represent the fraction of radiative transitions in the L_j subgroup connected with filling a vacancy in the L_i subshell, e.g., $F_{3\alpha} = \sum\Gamma_{3\alpha}/\Gamma_3$, where $\sum\Gamma_{3\alpha}$ is the sum of radiative widths which contribute to the $L\alpha$ subgroup emitted in the process of filling a vacancy in the $L3$ subshell.

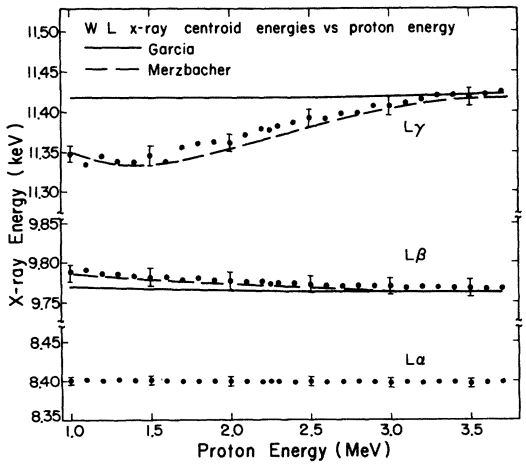

FIG. 11. $L\alpha$, $L\beta$, and $L\gamma$ centroid energies plotted vs proton energy for W. The BEA and PWBA predictions of Garcia and Merzbacher, respectively, are included for comparison.

When calculating the $L\alpha/Ll$ yield ratio, $I_{L\alpha}/I_{Ll}$, all factors in Eqs. (1) and (4) cancel except the $F_{3\alpha}$ and F_{3l}, leaving the predicted $L\alpha/Ll$ ratio as only $\sum\Gamma_{3\alpha}/\sum\Gamma_{3l}$, which is then obtained solely from Ref. 20. This simplification also occurs for the $K\alpha/K\beta$ predictions, since again only one subshell, $1s\frac{1}{2}$, is involved.

Figure 2 shows the Scofield predictions for $K\alpha/K\beta$ compared to the data. The measured values are, on the average, 10% low when compared to the calculation. Figures 4, 5, 7, and 8 show the PWBA and BEA predictions compared to our measured values for $L\alpha/L\beta$ and $L\alpha/L\gamma$ ratios. In general, the predictions reproduce the data qualitatively better than quantitatively. The BEA provides somewhat better fits to these ratios versus atomic number, while the PWBA better reproduces the general shape of the excitation functions. In Figs. 4 and 5, the BEA and PWBA predictions are not drawn as smooth curves but are instead shown as individual points for each element and energy. The calculations as a function of atomic number were not sufficiently continuous to justify a smooth curve drawn through the predicted points. This is due to the discontinuous nature of the f_{ij}'s and ω_i's as a function of atomic number (see Refs. 18 and 19). Figure 6 includes the predictions of Scofield for the $L\alpha/Ll$ ratios. The data and calculations are, generally, in good agreement, although the data error bars are large, making a quantitative comparison difficult.

As pointed out in Ref. 14, the subgroup centroid energies for $L\beta$ and $L\gamma$ can be predicted using the theoretical subshell cross sections. We calculated these centroid energies using the equations

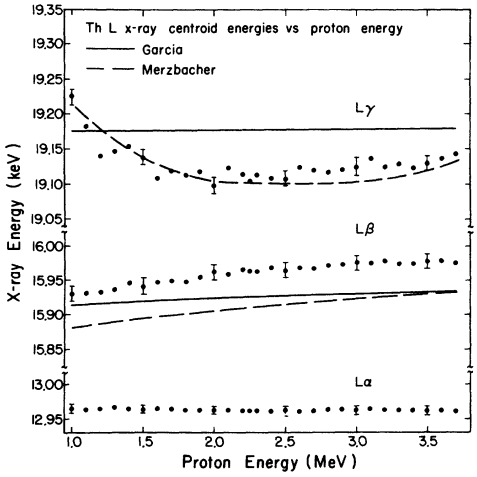

FIG. 12. $L\alpha$, $L\beta$, and $L\gamma$ centroid energies plotted vs proton energy for Th. The BEA and PWBA predictions of Garcia and Merzbacher, respectively, are included for comparison.

$$\bar{E}_{L\beta}=\{n_1\omega_1F_{1\beta}\bar{E}_{1\beta}+(n_1f_{12}+n_2)\omega_2F_{2\beta}\bar{E}_{2\beta}+[n_1(f_{13}+f_{12}f_{23})+n_2f_{23}+n_3]\omega_3F_{3\beta}\bar{E}_{3\beta}\}/I_{L\beta}\,, \tag{5}$$

and

$$\bar{E}_{L\gamma}=[n_1\omega_1F_{1\gamma}\bar{E}_{1\gamma}+(n_1f_{12}+n_2)\omega_2F_{2\gamma}\bar{E}_{2\gamma}]/I_{L\gamma}\,, \tag{6}$$

where, for example,

$$\bar{E}_{1\beta}=\frac{\sum_i\Gamma_{1\beta_i}E_{1\beta_i}}{\sum_i\Gamma_{1\beta_i}}$$

is the intensity-weighted average energy for the L_β component owing to a filled vacancy in the $L1$ subshell. The $\Gamma_{1\beta_i}$, etc., are the radiative widths of Scofield[20] and the $E_{1\beta_i}$, etc., are the measured energies[10] of the transitions.

As shown in Figs. 10–12, the BEA fails to provide the general shape of the centroid shifts for the $L\beta$ and $L\gamma$ centroid energies of Sm, W, and Th (note that the $L\alpha$ centroid energies remain constant, within ≤ 5 eV, with proton energy; this is, of course, predicted by both theories). The PWBA, however, better predicts the shape and magnitude of the centroid energies, especially for W.

A note should be added here concerning the sensitivity of the calculated yield ratios and centroid energies [Eqs. (1)–(6)] to the input parameters. A change of ± 20% in any one f_{ij}, ω_i, or σ_{Li} causes a change of less than 1% in $\bar{E}_{L\beta}$ and $\bar{E}_{L\gamma}$. For $L\alpha/L\beta$ or $L\alpha/L\gamma$, however, a change in any one f_{ij} or ω_1 of ± 20% causes a change of less than 5%. Moreover, a change of ± 20% in ω_2 or ω_3 can result in a change in $L\alpha/L\beta$ and $L\alpha/L\gamma$ of up to 20%. Ten percent changes in σ_{L2} or σ_{L3} result in these calculated ratios also varying nearly 10%. The calculations were performed with only one parameter changing at a time. Presumably, changing more than one parameter at a time could make larger changes in the resulting calculations. Therefore, in order to test the applicability of the BEA and PWBA theories, a highly reliable experimental set of f_{ij} and ω_i is essential. Such values are not presently available.

V. CONCLUSIONS

Both the PWBA and BEA give reasonable descriptions of the data and, as in the case of the cross-section measurements ($\sigma_{K\alpha}$ or $\sigma_{L\alpha}$) of Ref. 1, the BEA gives superior fits to the $L\alpha/L\beta$ and $L\alpha/L\gamma$ ratios of the present work. The PWBA, in general, does a reasonable job of providing a qualitative description of the data, with better pre-

dictions provided for the centroid energy shifts than are provided by the BEA. Some of the discrepancy in the BEA description may be due to the fact that the values for the L subshell ionization cross sections are derived[17] from the K-shell cross section for Mg, which has a different velocity distribution than does the L shell. Another factor in the over-all disagreement of the PWBA and BEA theories with the data is probably due to our choice of values for f_{ij} and ω_i. More complete experimental data on Koster-Kronig and fluorescence yields would be particularly useful.

---

†Work performed under the auspices of the U.S. Atomic Energy Commission.

*Visiting staff member from the University of Kansas, Lawrence, Kansas 66044.

[1]R. C. Bearse, D. A. Close, J. J. Malanify, and C. J. Umbarger, Phys. Rev. A 7, 1269 (1973).
[2]J. D. Garcia, Phys. Rev. A 1, 1 (1970).
[3]J. D. Garcia, Phys. Rev. A 1, 1402 (1970).
[4]G. S. Khandelwal, B. H. Choi, and E. Merzbacher, At. Data 1, 103 (1969) and corrected L subshell tables of the above; E. Merzbacher (private communication).
[5]Micro Matter Inc., 197 34th St. East, Seattle, Wash. 98102.
[6]E. J. Feldl and C. J. Umbarger, Nucl. Inst. Meth. 103, 341 (1972).
[7]G. A. Bissinger, S. M. Shafroth, and A. W. Waltner, Phys. Rev. A 5, 2046 (1972).
[8]J. L. Campbell and L. A. McNelles, Nucl. Inst. Meth. 98, 433 (1972).
[9]J. S. Hansen, J. C. McGeorge, D. Nix, W. D. Schmidt-Ott, I. Unus, and R. W. Fink, Nucl. Inst. Meth. 106, 365 (1973).
[10]J. A. Bearden, Rev. Mod. Phys. 39, 78 (1967).
[11]V. W. Slivinsky and P. J. Ebert, Phys. Rev. A 5, 1581 (1972).
[12]J. S. Hansen, H. U. Freund, and R. W. Fink, Nucl. Phys. A 142, 604 (1970).
[13]P. V. Rao, M. H. Chen, and B. Crasemann, Phys. Rev. A 5, 997 (1972).
[14]G. A. Bissinger, A. B. Baskin, B. H. Choi, S. M. Shafroth, J. M. Howard, and A. W. Waltner, Phys. Rev. A 6, 545 (1972).
[15]S. M. Shafroth, G. A. Bissinger, and A. W. Waltner, Phys. Rev. A 1, 566 (1973).
[16]C. E. Busch, A. B. Baskin, P. H. Nettles, S. M. Shafroth, and A. W. Walters, A 7, 1601 (1973).
[17]J. D. Garcia, latest calculated K-shell ionization cross sections for Mg (private communication).
[18]B. Crasemann, M. H. Chen, and V. O. Kostroun, Phys. Rev. A 4, 2161 (1971).
[19]M. H. Chen, B. Crasemann, and V. O. Kostroun, Phys. Rev. A 4, 1 (1971).
[20]J. H. Scofield, Phys. Rev. 179, 9 (1969).